

Foam in a two-dimensional Couette shear: a local measurement of bubble deformation.

E. JANIAUD^{1,2} and F. GRANER³ (*)

¹ *Laboratoire des Milieux Désordonnés et Hétérogènes, case 78, Université Paris 6 and CNRS UMR 7603, 4 place Jussieu, 75252 Paris Cedex 05, France.*

² *Université Paris 7, Denis Diderot, Fédération de Recherche FR2438 Matière et Systèmes Complexes, 2 place Jussieu, 75251 Paris Cedex 05, France.*

³ *Laboratoire de Spectrométrie Physique, CNRS UMR 5588 et Université Grenoble I, BP 87, F-38402 St Martin d'Hères Cedex, France.*

PACS. 83.80.Iz – Emulsions and foams.

PACS. 82.70.Rr – Aerosols and foams.

PACS. 83.50.-v – Deformation and flow.

PACS. 83.60.-a – Material behavior.

Abstract. – We re-analyse experiments of a two-dimensional foam sheared in Couette geometry [Debrégeas *et al.*, Phys. Rev. Lett. **87**, 178305 (2001)]. We characterise the bubble deformation by a texture tensor. Our measurements are local in time: they evidence the distinction between a transient regime and a permanent one, where we have access to both the average and fluctuations of the anisotropy. Moreover, the measurements are local in space and show that the deformation is not localised, varying smoothly across the shear gap.

Introduction. – A liquid foam exhibits a “complex” behaviour under stress: it is elastic at small deformation, plastic at large deformation, and flows at large deformation rate [1]-[7]. It is a model system, appropriate to study complex fluids: its typical length scales make it suitable for direct observation. In particular, a two-dimensional foam is easy to image, and image analysis yields information on all the geometrical properties of the foam.

Recently, Debrégeas *et al.* [8] have quasistatically sheared a two dimensional (2D) dry foam in a Couette geometry (Fig. 1, bottom left). They have studied the velocity field and showed that it is localised in a shear band. More precisely, the velocity decreases exponentially across the gap, as $\exp(-r/\lambda)$, where r is the distance to the inner wheel and λ is a characteristic length comparable to one bubble diameter. Such shear-bandin had been explained and numerically simulated by the combination of frozen disorder, elastic behaviour at low deformation, and local discrete plastic processes [9].

We would like to extract more physical information, beyond the velocity field. There have been various suggestions to quantify statistically the anisotropy and the deformation of the

(*) to whom correspondence should be addressed at graner@ujf-grenoble.fr

internal structure of the foam, that is, the bubble walls network. Most of them were based on scalar quantities, see for instance ref. [10]. Since the deformation encompasses information on both anisotropy and orientation, it is actually a tensorial quantity [11]. Recent suggestions of possible tensorial descriptions are promising [12, 13, 14]. Here, we use the “texture tensor” (eq. 1), which combines the following advantages [15]: (i) it is purely geometrical, independent from stresses and forces; (ii) it applies to any small or large number of bubbles; (iii) it is local in time and space [16], thus can characterise a sub-region of the foam.

In this letter, we first briefly present the original experimental set-up, and our image analysis protocol. We then present two analyses of experiments. The first one, resolved in both time and space, studies the transient regime before a stationary flow is established. The second, resolved in space (and averaged in time), shows that in the stationary flow the bubble anisotropy varies smoothly across the Couette gap and is not localised near the inner rotating wheel.

Experiments. – Experimental data were generously provided by Georges Debrégeas. They were obtained in two different runs. The experimental set-up has been described in details in Ref. [8]. Briefly, it consisted in an inner shearing wheel and an outer wheel (of respective radii: $R_0 = 71$ mm; and R_1 , different for each run) confined between two transparent plates separated by 2 mm spacers. This foam thickness was smaller than the distance between bubbles (see below), ensuring that there was only one layer of bubbles (no 2D \rightarrow 3D transition [17]). The fluid fraction, measured by the weight of water introduced in the cell, was $\Phi = 5.2\%$. Coarsening and size sorting under shear were negligible during the experiment. To reduce the effect of viscous friction between the bubbles and the confining plates, the inner wheel rotated at velocity $V_{wheel} = 0.25$ mm.s $^{-1}$. This was well in the quasistatic regime; results presented below are thus expressed as function, not of the time t , but rather of the applied shear $\gamma = V_{wheel} t / (R_1 - R_0)$. The position and the shape of the bubbles were recorded by a CCD digital camera. To prepare the foam, the inner disc was rotated clockwise until a stationary regime was reached: then, at an arbitrary time, which was chosen as the origin ($t = \gamma = 0$), the shear direction was switched to counter-clockwise and the experiment began.

Run 1 (unpublished data) started at $\gamma = 0$ and thus contained a transient regime. The average distance between (the centres of mass of) neighbour bubbles was 3.0 mm, with a standard deviation of ± 0.5 mm; this corresponded to a mean bubble wall length of $\langle \ell \rangle = 1.7$ mm. The external radius was $R_1 = 112$ mm. Thus $\gamma = 1$ corresponded to a wheel displacement of $V_{wheel} t = R_1 - R_0 = 41$ mm: *i.e.* 15-20 bubble diameters. 500 pictures were recorded, each showing 200 bubbles.

Run 2 (published in Ref. [8]) focussed on a stationary regime. The average distance between (the centres of mass of) neighbour bubbles was 2.4 mm, with a standard deviation of ± 0.4 mm; this corresponded to a mean bubble wall length of $\langle \ell \rangle = 1.4$ mm. The external radius was $R_1 = 122$ mm. Thus $\gamma = 1$ corresponded to a wheel displacement of 51 mm: *i.e.* 20-25 bubbles diameters. Before recording data, a full 2π -turn was performed, corresponding to $\gamma = 8$. A quarter of the cell was filmed, with 700 bubbles on each picture. To improve the statistics, the camera was then displaced to record successively the four quarters. 2000 pictures were obtained as four 500-images movies.

Image analysis. – We analyse the images using a home-made extension module to the public software NIH-Image. We binarise the image by thresholding, and skeletise the bubble walls to a one pixel thickness. We identify the points where three walls meet (“vertices”). We replace each wall by the vector linking its vertices (white lines on Fig. 1a, top right).

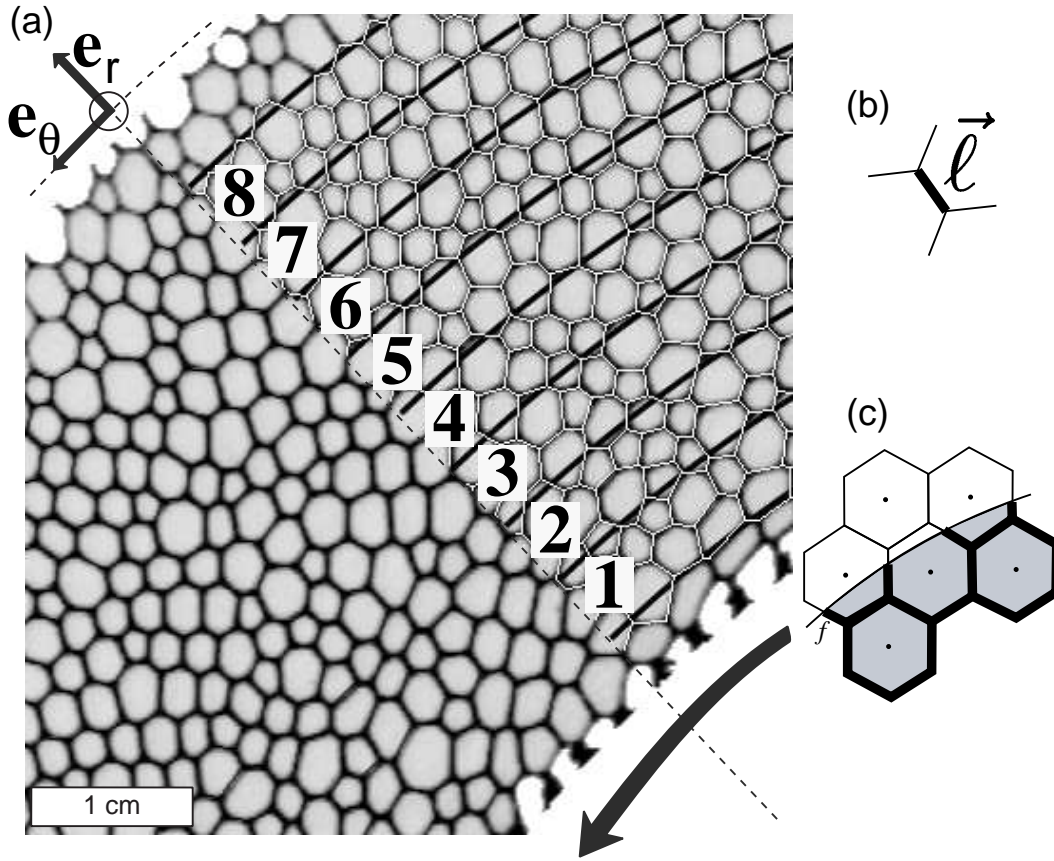


Fig. 1 – (a) Foam under steady quasistatic shear in a two-dimensional (2D) Couette geometry. *Bottom left*: top view of the original experiment by Debrégeas *et al.* [8]. The foam was enclosed between two horizontal glass plates. The inner wheel turned counter-clockwise and, due to its tooth-shaped boundaries, carried the first row of bubbles with no-slip conditions. The outer wheel remained fixed. *Top right*: image analysis. The reconstructed network of vertices linked by vectors (white) and the boundaries of the 8 equi-spaced concentric boxes used for spatial analysis (black arcs of circle) are superimposed on the snapshot of the experiment. We exclude the regions near both disks, where the bubbles are not entirely visible. (b) We denote by $\vec{\ell}$ the vector linking both vertices of a given wall. (c) If one of these vertices is outside of the box (defined in (a), top right), we denote by f the fraction of the wall inside the box.

These wall vectors $\vec{\ell}$ (Fig. 1b) are expressed in local polar coordinates (Fig. 1a) to respect the symmetry of the Couette cell. For the same reason, we chose equi-spaced orthoradial boxes (Fig. 1, top right) to divide the foam and measure the deformation. For Run 1, each box is $2.7\langle\ell\rangle$ wide, and the box number i is at distance $r_1^i = [0.4 + 2.7(i - 0.5)]\langle\ell\rangle$ from the inner wheel. For Run 2, $r_2^i = [2.8 + 3.1(i - 0.5)]\langle\ell\rangle$. We do not take into account the walls which are too close from each wheel.

To quantify the anisotropy of each region of the foam, we proceed as follows. We want to characterise statistically the pattern of the walls $\vec{\ell}$. More precisely, we want to take into account the direction and the length ℓ of the walls; however, since the symmetry $\vec{\ell} \rightarrow -\vec{\ell}$ does not affect the pattern, the orientation of $\vec{\ell}$ should play no role in what follows. We first

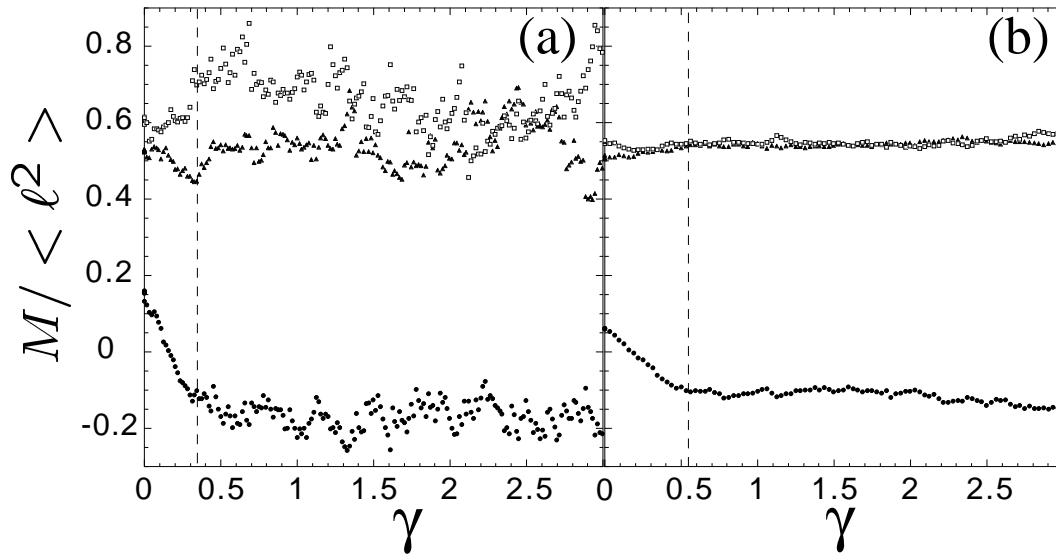


Fig. 2 – Run 1: components of the texture tensor $\overline{\overline{M}}$ for the first 200 images (closed triangles : M_{rr} ; open squares: $M_{\theta\theta}$; closed circles: $M_{r\theta}$) versus the applied shear γ . The components have been normalised by the average length of the bubble wall, $\langle \ell^2 \rangle$. (a) Innermost box number 1; (b) outermost box number 8; The dashed line represents the cross-over γ_C between the transient and stationary regimes.

construct, for each wall, the tensor $\vec{\ell} \otimes \vec{\ell}$: its coordinates are $(\ell_i \ell_j)$, where i, j are here r or θ . In each given box, we then measure the local “texture tensor” [15], $\overline{\overline{M}}$, which reflects at large scales the relevant features (average size, anisotropy) of the actual microstructure of the material (Fig. 1a):

$$\overline{\overline{M}} = \left\langle f \vec{\ell} \otimes \vec{\ell} \right\rangle = \left\langle f \begin{pmatrix} \ell_r^2 & \ell_\theta \ell_r \\ \ell_r \ell_\theta & \ell_\theta^2 \end{pmatrix} \right\rangle, \quad (1)$$

where $\langle \cdot \rangle$ denotes the average over all walls. Here, walls are weighted by their fraction f inside this box ($0 \leq f \leq 1$), see Fig. (1c): this procedure is not crucial, since weighted and unweighted averages yield similar results. The diagonal components M_{rr} and $M_{\theta\theta}$ of this tensor are both of order $\langle \ell^2 \rangle$. Conversely, the off-diagonal component $M_{r\theta} = M_{\theta r}$ (the tensor is symmetric) is much smaller, and even vanishes when the foam is isotropic. Hence the tensor $\overline{\overline{M}}$ has two strictly positive eigenvalues, also of order $\langle \ell^2 \rangle$, the largest being in the direction in which bubbles elongate. It thus quantifies the anisotropy and the dilation of the network consisting of the bubble vertices.

Results. – Run 1 displays two distinct regimes: a transient and a stationary flow (Fig. 2).

In the *transient regime*, the average wall length does not change much, but the walls tend to align with the direction of the rotation. Hence, only the crossed component $M_{r\theta}$ is correlated to the shear. Since $\gamma = 0$ marks the change from clockwise to counter-clockwise shear, $M_{r\theta}$ decreases linearly and progressively changes sign. No bubble rearrangement (“T1 process”) is visible: this probably correspond to the elastic regime [2].

At a critical shear γ_C , there is a cross-over to the *stationary flow*. The value of γ_C increases

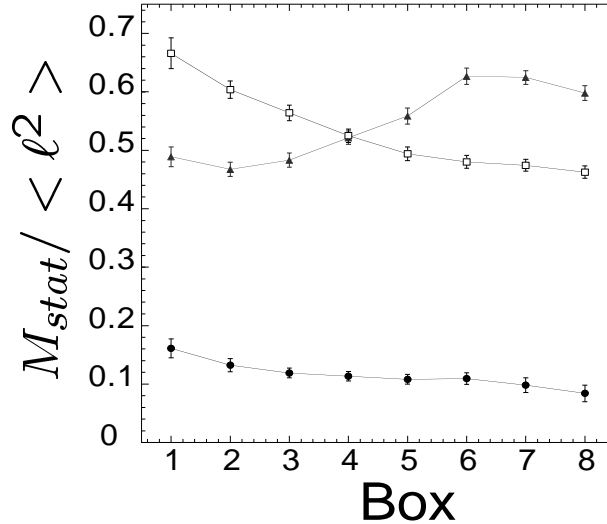


Fig. 3 – Run 2: stationary flow. The components of the texture tensor $\overline{\overline{M}}$ (closed triangles: M_{rr} ; open squares: $M_{\theta\theta}$; closed circles: $M_{r\theta}$) again normalised by $\langle \ell^2 \rangle$, are averaged over the four quarters of the whole foam, but also over time (2000 pictures).

gradually (data not shown, see [18]) from 0.35 for the inner box (Fig. 2a), to 0.55 for the outer box (Fig. 2b). In the stationary regime, the components of the texture tensor are fluctuating around a mean value. The texture tensor provides a good tool to study these time fluctuations and their correlations (data not shown, see [18, 19]). The short-term fluctuations are much larger near the inner wheel (Fig. 2a) than near the outer one (Fig. 2b): these fluctuations might be linked to the velocity gradient, which includes both elastic and plastic deformations (T1 processes) [8]. No avalanche-like events [7] are visible on these figures (nor on the histograms of the texture tensor increments: positive and negative increments have similar frequencies, data not shown, see [18]).

Run 2 allows us to improve the statistics, using temporal averages over the stationary flow. Not only can we detect the anisotropy of the foam, $M_{r\theta}$, barely visible by eye on the original picture (Fig. 1), but we can also detect its tiny variations in space (Fig. 3). Surprisingly, we detect in the outer boxes a non-zero anisotropy, visible as a difference between M_{rr} and $M_{\theta\theta}$ on average over the whole foam. This deformation is likely a trace of the procedure used to fill the cell with foam [8], which the initial clockwise shear does not suffice to relax [20].

$M_{r\theta}$ is larger in the inner boxes than in the outer ones, reflecting the preferred orientation imposed by the shear. Interestingly, $M_{r\theta}$ is not localised near the inner wheel: its decrease with the distance to the inner wheel is smooth.

Conclusion. – In this letter, we use a recently introduced tool, the texture tensor $\overline{\overline{M}}$ [15], to characterise statistically the anisotropy of a foam, here in a quasistatic 2D Couette shear [8]. It allows to distinguish two different regimes as shear increases: first, a transient regime where the cross component increases linearly with shear; second, a stationary regime where all component are fluctuating around a mean value.

We have shown that the average of $\overline{\overline{M}}$ is suitable to describe the anisotropy of the sheared foam pattern. It even quantifies some features of the foam which are indistinguishable by

eye: for instance, the preparation-dependent anisotropy of the foam, which is retained in the outermost regions.

The variation of \overline{M} with shear does not display any avalanche-like fluctuations; its variations with space does not exhibit any sign of localisation. This contrasts strongly with the velocity field, measured on the same Run 2 [8], which displays a clear localisation near the inner wheel: as mentioned above, it decreases exponentially, over a length comparable to a bubble diameter. The texture tensor can be used to characterise the geometry of a variety of 2D and 3D disordered networks of vertices [11]. It allows to treat a microscopically discrete medium as continuous at mesoscopic scales. For instance, it has been used to measure *in situ* the shear modulus of 2D foams [21, 22]. It could be applied to 3D foams (each vertex being the meeting point of four bubbles faces), but also to grain boundaries in crystals [23], granular media (each vertex being a grain center), and even 2D epithelial tissues or 3D aggregates of biological cells.

* * *

We are extremely grateful to G. Debrégeas for providing us with many recordings of his published and unpublished experiments, and for detailed discussions. We would also like to thank M. Asipauskas, M. Aubouy, O. Cardoso, F. Elias, J.A. Glazier, Y. Jiang, A. Kabla, J. Scheibert for discussions and support, F. Elias for critical reading of the manuscript. This work was partially supported by CNRS ATIP 0693.

REFERENCES

- [1] WEAIRE D. and HUTZLER S., *Physics of Foams* (Oxford Univ. Press, Oxford) 1999.
- [2] HÖHLER R., COHEN-ADDAD S. and HOBALLAH H., *Phys. Rev. Lett.*, **79** (1997) 1154.
- [3] DURIAN D. J., *Phys. Rev. E*, **55** (1997) 1739.
- [4] LAURIDSEN J., TWARDOS M. and DENNIN M., *Phys. Rev. Lett.*, **89** (2002) 098303.
- [5] YBERT C. and DI MEGLIO J.-M., *C.R. Physique*, **3** (2002) 555.
- [6] PRATT E. and DENNIN M., preprint, 2003.
- [7] JIANG Y., SWART P.J., SAXENA A., ASIPAUSKAS M. and GLAZIER J.A., *Phys. Rev. E*, **59** (1999) 5819.
- [8] DEBRÉGEAS G., TABUTEAU H. and DI MEGLIO J.-M., *Phys. Rev. Lett.*, **87** (2001) 17-8305.
- [9] KABLA A. and DEBRÉGEAS G., preprint, cond-mat/021164v1 (2002).
- [10] ELIAS F., FLAMENT C., GLAZIER J. A., GRANER F. and JIANG Y. , *Philos. Mag. B*, **79** (1999) 729.
- [11] ALEXANDER S., *Phys. Reports*, **296** (1998) 65.
- [12] REINELT D. A. and KRAYNIK A., *J. Rheology*, **44** (2000) 453.
- [13] KRAYNIK A., REINELT D., VAN SWOL F., preprint (2002).
- [14] BALL R. and BLUMENFELD R., *Phys. Rev. Lett.*, **88** (2002) 115505.
- [15] AUBOUY M., JIANG Y., GLAZIER J. A. and GRANER F., *Granular Matt.*, (2003) to appear, cond-mat/0301018.
- [16] JIANG Y., ASIPAUSKAS M., GLAZIER J. A., AUBOUY M. and GRANER F., *Eurofoam 2000*, edited by P. ZITHA, J. BANHART, G. VERBIST (MIT Verlag, Bremen) 2000, p. 297.
- [17] COX S.J., WEAIRE D., and VAZ M.F., *Eur. Phys. J. E*, **7** (2002) 311.
- [18] JANIAUD E., PhD thesis, Univ. Paris 7, in preparation (2003).
- [19] SCHEIBERT J., DEBRÉGEAS G., in preparation.
- [20] DEBRÉGEAS G., private communication.
- [21] ASIPAUSKAS M., AUBOUY M., JIANG Y., GRANER F. and GLAZIER J.A., *Granular Matt.*, (2003) to appear, cond-matt /0301017.

- [22] COURTY S., DOLLET B., ELIAS F., HEINIG P. and GRANER F., 2003preprint, cond-mat/0305408.
- [23] DURAND G., WEISS J., GRANER F., in preparation.